FUSE

Fungal Systematics and Evolution

VOLUME 4
DECEMBER 2019
PAGES 171–181

doi.org/10.3114/fuse.2019.04.09

Fusarium volatile, a new potential pathogen from a human respiratory sample

A.M.S. Al-Hatmi[1,2,3*], M. Sandoval-Denis[1,4], C. Nabet[5], S.A. Ahmed[1,2,6], M. Demar[7], A.-C. Normand[5], G.S. de Hoog[1,2,8]

[1]Westerdijk Fungal Biodiversity Institute, P.O. Box 85167, 3508 AD Utrecht, The Netherlands
[2]Foundation Atlas of Clinical Fungi, Hilversum, The Netherlands
[3]Ministry of Health, Directorate General of Health Services, Ibri, Oman
[4]Faculty of Natural and Agricultural Sciences, Department of Plant Sciences, University of the Free State, South Africa
[5]Sorbonne Université, INSERM, Institut Pierre-Louis d'Epidémiologie et de Santé Publique, AP-HP, Groupe Hospitalier Pitié-Salpêtrière, Service de Parasitologie-Mycologie, F-75013, Paris, France
[6]Faculty of Medical Laboratory Sciences, University of Khartoum, Khartoum, Sudan
[7]Laboratoire Hospitalo-Universitaire de Parasitologie-Mycologie Centre Hospitalier Andrée Rosemon, Cayenne, French Guiana
[8]Centre of Expertise in Mycology Radboud University Medical Centre / Canisius Wilhelmina Hospital, Nijmegen, The Netherlands

*Corresponding author: a.alhatmi@gmail.com

Key words:
clinical samples
FFSC
French Guiana
fungal taxonomy
phylogeny

Abstract: We describe the isolation and characterization of *Fusarium volatile* from a bronchoalveolar lavage (BAL) sample of a female patient living in French Guiana with underlying pulmonary infections. Phylogenetic analysis of fragments of the calmodulin (*cmdA*), translation elongation factor (*tef1*), RNA polymerase second largest subunit (*rpb2*), and β-tubulin (*tub*) loci revealed that strain CBS 143874 was closely related to isolate NRRL 25615, a known but undescribed phylogenetic species belonging to the African clade of the *Fusarium fujikuroi* species complex. The fungus differed phylogenetically and morphologically from related known species, and is therefore described as the new taxon *Fusarium volatile*. Antifungal susceptibility testing suggested that the new species is resistant to echinocandins, fluconazole, itraconazole with lower MICs against amphotericin B, voriconazole and posaconazole.

Effectively published online: 25 June 2019.

INTRODUCTION

Species of the *fujikuroi* species complex (FFSC) of the genus *Fusarium* have been extensively studied in view of their ability to cause infections in plants and to produce toxins that may lead to food poisoning (Chilaka *et al*. 2017). Moreover, some members of the FFSC have repeatedly been reported from opportunistic infections in humans, which may be mild or local in the case of onychomycosis and keratitis, or invasive and severe in individuals with extended burn wounds and bone marrow transplant recipients. In addition, systemic and disseminated infections occur in severely immunocompromised patients (Guarro 2013, Al-Hatmi *et al*. 2016b, de Hoog *et al*. 2019).

The FFSC is one of the larger groups within the genus *Fusarium* and contains species with diverse ecologies (Nirenberg & O'Donnell 1998, O'Donnell *et al*. 2000). Species of the FFSC are characterised by forming yellow, orange or purple colonies on potato dextrose agar (PDA); globose, oval, napiform or clavate microconidia are borne in chains and false heads on mono- and polyphialides, while different combinations of microconidial morphologies and phialide types can coexist; the macroconidia are thin-walled, almost straight to slightly curved, with a well-developed pedicellate basal cell. Chlamydospores are rarely formed in the FFSC, although they can be present in some species, formed mostly intercalarily on the hyphae, grouped in chains or clusters (Nirenberg & O'Donnell 1998, Leslie & Summerell 2006).

Molecular studies suggested that at least 50 phylogenetic lineages may be recognized within FFSC. Three major clades with limited biogeographic distribution can be distinguished, and these are termed the African, American and Asian clades (O'Donnell *et al*. 1998). Thus far 16 species of the FFSC have been reported to cause human infections, namely *F. acutatum*, *F. ananatum*, *F. andiyazi*, *F. anthophilum, F. fujikuroi*, *F. guttiforme*, *F. musae*, *F. napiforme*, *F. nygamai*, *F. proliferatum*, *F. ramigenum*, *F. sacchari*, *F. subglutinans*, *F. temperatum*, *F. thapsinum* and *F. verticillioides* (Al-Hatmi *et al.* 2016a, de Hoog *et al*. 2019).

Identification to species level in FFSC is often difficult because of the high morphological diversity and intraspecific variation of microscopic features (O'Donnell *et al*. 2015). Currently known species of the FFSC are morphologically and genetically very similar and often can only be reliably separated using multilocus molecular analyses (Geiser *et al.* 2004). However, considering that some members of the FFSC are relevant human opportunistic pathogens or important toxin producers, their correct identification is crucial. The present paper describes a species of FFSC, based on isolate CBS 143874 collected from a human patient specimen in Cayenne, French Guiana, and characterised by morphological and phylogenetic methods. A morphological identification key is provided to identify the novel species and additional FFSC species known from human clinical specimens.

CASE REPORT

The patient was a 22-yr-old woman, native of Brazil, but has lived in French Guiana for 8 yr. She presented at the Internal Medicine Department of the Andrée Rosemon hospital centre in Cayenne (French Guiana) with a 4-mo history of chronic asthenia at the moment of clinical examination. A right cervical, sub-angulomaxillary adenophlegmon had appeared 1 mo earlier. She did not have any other clinical signs and had no cough or weight loss and denied night sweats. She had antecedents of disseminated lupus erythematous diagnosed a year before and was treated with an association of hydroxychloroquine and corticoids. Corticotherapy had been interrupted 4 mo earlier.

Chest computed tomography revealed the presence of a left apical pulmonary cavern with alveolar opacity. Computed tomography of the head and neck highlighted the presence of several cervical necrotic adenomegalies on the right side associated with an abscessed subcutaneous collection. Inflammatory syndrome was mild (C-reactive protein = 7 mg/L). A chest radiography suggested the presence of an aspergilloma, with an image compatible with an *Aspergillus* ball into the pulmonary cavern.

Presence of bacteria and fungi was assessed by culturing a broncho-alveolar fluid (BAL) sample. Cultures were negative for bacterial growth including mycobacteria. Cultures for fungi were positive for a fusarium-like fungus. Although there was no evidence of bacterial infection, the patient was diagnosed as having a tuberculosis adenitis based on the presence of a pulmonary cavern at radiography. She was treated with the following antituberculosis quadritherapy (Ethambutol, Isoniazide, Pyrazinamide and Rifampicine). *Fusarium* growth was not taken into consideration due to the absence of pulmonary and systemic clinical signs. Patient evolution under treatment was spectacular with a rapid regression of adenitis and a diminution of the asthenia. At 6 mo, lesions had completely disappeared at computed tomography. The *Fusarium* isolate was sent to the Westerdijk Fungal Biodiversity Institute (WI), Utrecht, The Netherlands, for further characterization.

MATERIALS AND METHODS

Strains

A *Fusarium* sp. strain was isolated from BAL fluid specimen of the patient in French Guiana and submitted to the WI, under accession number CBS 143874. Ex-type and reference strains spanning the known diversity of the FFSC were selected based on phylogenetic and morphological similarity to the strain under study (Table 1). The clinical isolate was grown on PDA slants for 7 d at 25 °C, and was maintained as working culture or stored in 20 % (v/v) glycerol at -80 °C for prolonged use.

Table 1. GenBank accession numbers of *Fusarium* species included in this study.

				GenBank/ENA accession number[2]			
Species	**Collection[1]**	**Source**	**Country**	***cmdA***	***rpb2***	***tef1***	***tub***
F. agapanthi	NRRL 54463^{T}	*Agapanthus praecox*	Australia	KU900611	KU900625	KU900630	KU900635
	NRRL 54464	*Agapanthus praecox*	Australia	KU900613	KU900627	KU900632	KU900637
F. ananatum	CBS 118516^{T}	*Ananas comosus* fruit	South Africa	LT996175	LT996137	LT996091	LT996112
	CBS 118517	*Ananas comosus* fruit	South Africa	KU603990	KU604273	KU604480	KU603895
F. andiyazi	CBS 119857^{T}	*Sorghum bicolor* soil debris	South Africa	LT996176	LT996138	LT996092	LT996113
	CBS 134430	Human	Turkey	KU603956	KU604232	KU604450	KU603867
F. anthophilum	CBS 737.97	*Hippeastrum* sp.	Germany	LT996177	LT996139	LT996093	LT996114
	CBS 119859	*Cymbidium* sp. leaf spot	New Zealand	KU603988	KU604279	KU604427	KU603931
F. bactridioides	NRRL 20476	*Cronartium conigenum*	USA	AF158343	-	AF160290	U34434
F. begoniae	CBS 403.97	*Begonia elatior* hybrid	Germany	AF158346	LT996140	AF160293	U61543
	NRRL 31848	*Begonia elatior* hybrid	USA	-	-	AY329035	AY329044
F. bulbicola	CBS 220.76^{T}	*Nerine bowdenii*	Germany	KF466327	KF466404	KF466415	KF466437
F. circinatum	CBS 405.97^{T}	*Pinus radiata*	USA	KM231393	HM068354	KM231943	KM232080
F. coicis	NRRL 66233^{T}	*Coix gasteenii*	Australia	LT996178	KP083274	KP083251	LT996115
F. ficicrescens	CBS 125178^{T}	*Ficus carica* fruit	Iran	KU603958	KT154002	KU604452	KP662896
	CBS 125181	*Ficus carica* fruit	Iran	KU603959	KT154003	KU604453	KP662897
F. lactis	CBS 411.97^{NT}	*Ficus carica*	USA	AF158325	LT996149	AF160272	U61551
	NRRL 31630	*Capsicum annuum*	Belgium	FR870301	FR870313	FR870289	FR870325
F. mexicanum	NRRL 47473	*Mangifera indica* inflorescence	Mexico	GU737389	Not public	GU737416	GU737308
	NRRL 53580	*Mangifera indica* inflorescence	Mexico	GU737394	-	GU737421	GU737367
F. nygamai	NRRL 13448^{T}	Necrotic *Sorghum* root	Australia	AF158326	EF470114	AF160273	U34426
	NRRL 26421	Human	Egypt	KU603949	EF470127	HM347121	KU603865
F. oxysporum	CBS 716.74	*Vicia faba*	Germany	AF158366	JX171583	AF008479	U34435
	CBS 744.97	*Pseudotsuga menziesii*	USA	AF158365	LT575065	AF160312	U34424
F. phyllophilum	CBS 216. 76^{T}	*Dracaena deremensis* leaf	Italy	KF466333	KF466410	KF466421	KF466443

Table 1. (Continued).

Species	Collection[1]	Source	Country	GenBank/ENA accession number[2]			
				cmdA	*rpb2*	*tef1*	*tub*
F. pseudocircinatum	CBS 449.97[T]	*Solanum* sp.	Ghana	AF158324	LT996151	AF160271	U34427
F. pseudonygamai	CBS 417.97[T]	*Pennisetum typhoides*	Nigeria	AF158316	LT996152	AF160263	U34421
F. ramigenum	CBS 418.98[T]	*Ficus carica*	USA	KF466335	KF466412	KF466423	KF466445
Fusarium sp.	NRRL 25346	Pine pitch canker	USA	AF158349	-	AF160296	U61642
	NRRL 26756	Plant leaf litter	Cuba	AF158360	Not public	AF160307	AF160336
	NRRL 26757	Pine pitch canker	USA	AF158361	-	AF160308	AF160351
F. subglutinans	CBS 747.97	*Zea mays*	USA	AF158342	JX171599	AF160289	U34417
F. sudanense	CBS 454.97[T]	*Striga hermonthica*	Sudan	LT996185	LT996155	KU711697	KU603909
F. temperatum	NRRL 25622	*Zea mays*	South Africa	AF158354	Not public	AF16030	AF160317
F. terricola	CBS 483.94[T]	Soil	Australia	KU603951	LT996156	KU711698	KU603908
F. thapsinum	CBS 733.97	*Sorghum bicolor*	South Africa	LT996186	JX171600	AF160270	U34418
F. tjaetaba	NRRL 66243[T]	*Sorghum interjectum*	Australia	LT996187	KP083275	KP083263	GU737296
F. udum	NRRL 22949	*Lactarius pubescens*	Germany	AF158328	LT996172	AF160275	U34433
F. verticillioides	CBS 734.97	*Zea mays*	Germany	AF158315	EF470122	AF160262	U34413
	CBS 115135	Human	Sweden	KU603944	KU604217	KU604384	KU603861
F. volatile	CBS 143874[T]	Human bronchoalveolar lavage fluid	French Guiana	MK984595	LR596006	LR596007	LR596008
	NRRL 25615	*Oryza sativa* seed	Nigeria	AF158357	-	AF160304	AF160348
F. werrikimbe	CBS 125535[T]	*Sorghum leiocladum*	Australia	-	-	EF107131	EF107133
	F19361	*Sorghum leiocladum*	Australia	-	-	EF107132	EF107134
F. xylarioides	NRRL 25486[T]	*Coffea* trunk	Ivory Coast	-	HM068355	AY707136	AY707118

[1] CBS: Westerdijk Fungal Biodiverity Institute, Utrecht, The Netherlands. F: University of Sydney, Sydney, New South Wales, Australia. NRRL: Agricultural Research Service Culture Collection, National Center for Agricultural Utilization Research, USDA, Peoria, IL, USA. [NT]: ex-neotype. [T]: ex-type.

[2] ENA: European Nucleotide Archive. *cmdA*: calmodulin. *rpb2*: RNA polymerase second largest subunit. *tef1*: translation elongation factor–alpha. *tub*: β-tubulin. Sequences marked as *Not public* are available on the sequence datasets published by Edwards *et al.* (2016).

Morphology

CBS 143874 was characterised morphologically following procedures described elsewhere (Aoki *et al*. 2013, Leslie & Summerell 2006, Sandoval-Denis *et al.* 2018). Colony growth rates and production of diffusible pigments were evaluated on PDA, colony features were also recorded on malt extract agar (MEA) and oatmeal agar (OA). Colour notations followed those of Rayner (1970). Micro-morphological features were studied from cultures grown for 7–10 d at 24 °C, using a 12 h light/dark cycle with near-UV and white fluorescent light. Features of the aerial and sporodochial conidiophores, conidia and production of chlamydospores were assessed on synthetic nutrient-poor agar (SNA; Nirenberg 1976) and on carnation leaf agar (CLA; Fisher *et al*. 1982). Measurements and photomicrographs were recorded using sterile water as mounting medium and a Nikon Eclipse 80i (Nikon, Tokyo, Japan) microscope with Differential Interference Contrast (DIC) optics and a Nikon AZ100 dissecting microscope, both equipped with a Nikon DS-Ri2 or a Nikon DS-5 high definition colour digital camera and the Nikon software NIS-elements D software v. 4.30.

Growth rates

Cardinal growth temperatures were determined on MEA and PDA plates incubated in the dark for 2 wk at temperatures of 18–40 °C at intervals of 3 °C; with two replicates for each isolate. Average growth rates per species were calculated and expressed as diametric growth per 24 h.

DNA extraction, amplification and sequencing

The Wizard® Genomic DNA purification Kit (Promega, Madison, WI, USA) was used to extract total genomic DNA from fresh mycelium scraped from the surface of 7-d-old cultures on MEA at 24 °C. Partial fragments of four loci were PCR-amplified following previously published protocols using the following primer pairs: BT-2a/BT-2b for the β-tubulin gene (*tub*) (Glass & Donaldson 1995), CL1/CL2 for the calmodulin gene (*cmdA*) (O'Donnell *et al.* 2009), EF-1/EF-2 for the translation elongation factor-alpha gene (*tef1*) (O'Donnell *et al.* 1998), and RPB2-5f2/7cr plus RPB2-7cf/11ar for two non-contiguous fragments of the RNA polymerase second largest subunit (*rpb2*) (Liu *et al.* 1999, Sung *et al.* 2007). Sequencing was done in both directions using the respective PCR primers on an Applied Biosystems 3730xl DNA Analyzer (Life Technologies, Carlsbad, CA, USA). The DNA sequences were analysed and consensus sequences were assembled using SeqMan Pro v. 13 (DNAStar, Madison, WI, USA).

Phylogenetic analyses

Phylogenetic analyses of single loci and the combined dataset were carried out using three independent algorithms: Maximum-likelihood (ML), Maximum Parsimony (MP) and Bayesian

Table 2. MIC values of clinical isolate CBS 143874 (µg/mL).

Strain	AMB	FLC	ITC	VOR	POS	ISA	ANI	MICA
CBS 143874	1	>64	>16	1	0.5	4	>8	>8

AMB: amphotericin B. FLC: fluconazole. ITC: itraconazole. VOR: voriconazole. POS: posaconazole. ISA: isavuconazole. ANI: anidulafungin. MICA: micafungin.

inference (BI). Both ML and BI were run on the CIPRES Science Gateway portal (Miller *et al*. 2012). Evolutionary models were calculated with MrModelTest v. 2.3 using the Akaike information criterion (Nylander 2004). For ML, RAxML-HPC2 v. 8.2.10 on XSEDE was used (Stamatakis 2014), with a bootstrap analysis (BS) based on default parameters. The BI analyses were run using MrBayes v. 3.2.6 on XSEDE (Ronquist & Huelsenbeck 2003) using four incrementally heated MCMC chains for 5 M generations and a sample frequency of every 1 000 trees. The 50 % consensus trees and posterior probabilities (PP) values were calculated after discarding the first 25 % of samples as burn-in. Maximum-parsimony analyses were run using PAUP v. 4.0b10 (Swofford 2003). Heuristic searches included 1 000 random stepwise addition replicates, with tree bisection and reconstruction (TBR) branch swapping; all characters were equally weighted and gaps treated as missing data. Branches of zero length were collapsed and all multiple, equally parsimonious trees were saved. Tree statistics [tree length (TL), consistency index (CI), retention index (RI) and rescaled consistency index (RC)] were calculated. Clade stability was evaluated using a bootstrap analysis (BS) of 1 000 replicates.

Antifungal susceptibility

Antifungal susceptibility testing of CBS 143874 was performed by the CLSI broth microdilution as described in the CLSI document M38-A2 (Clinical and Laboratory Standards Institute 2008) with modifications according to Al-Hatmi *et al.* (2015). The following drugs were used: amphotericin B (Sigma-Aldrich), fluconazole (Pfizer, Groton, CT, USA), itraconazole (Janssen Pharmaceutica, Tilburg, The Netherlands), voriconazole (Pfizer), posaconazole (Merck), isavuconazole (Basilea Pharmaceutica, Basel, Switzerland), micafungin (Astellas, Ibaraki, Japan), and anidulafungin (Pfizer). Three reference strains (*Paecilomyces variotii* ATCC 22319, *Candida krusei* ATCC 6258, and *Candida parapsilosis* ATCC 22019) were included as quality controls.

RESULTS

Molecular analyses

Topologies obtained from the analyses of the majority of individual gene datasets were congruent, differing only in the positions of unsupported nodes. Individual analyses of the *cmdA*, *rpb2*, *tef1* and *tub* loci consistently resolved *Fusarium* sp. CBS 143874 as a member of the African clade *sensu* O'Donnell *et al.* (1998) (Fig. 1). Phylogenies based on *cmdA*, *rpb2* and *tef* sequences showed that strain CBS 143874, together with an unidentified isolate (NRRL 25615) formed a genetically exclusive lineage, phylogenetically related to *F. coicis* and *F. verticillioides*. In contrast, the *tub* phylogeny failed to unambiguously identify most of the *Fusarium* species included in this study, showing mostly marginal statistical support values that did not allow unequivocal separation of lineages. Nevertheless, this locus confirmed the phylogenetic position of CBS 143874 and NRRL 25615 as close relatives of *F. coicis*. With the exception of *tub*, single locus phylogenies did not support the monophyly of the African clade of FFSC, which resolved as polyphyletic.

The final, combined alignment encompassed a total of 3 305 positions (*cmdA* 545, *rpb2* 1 591, *tef1* 680, *tub* 489), of which 696 sites were variable (*cmdA* 86, *rpb2* 295, *tef1* 194, *tub* 121) and 452 were phylogenetically informative (*cmdA* 61, *rpb2* 204, *tef1* 119, *tub* 68). The combined phylogeny confirmed the results of the individual phylogenetic analyses, *Fusarium* sp. strains CBS 143874 and NRRL 25615 formed a highly-supported, genetically exclusive group, closely related to but different from *F. coicis* and *F. verticillioides* (Fig. 2); consequently, the above-mentioned phylogenetic clade is proposed here as the new species *Fusarium volatile*.

Antifungal susceptibility testing

Antifungal susceptibility testing according to CLSI M38A (Clinical and Laboratory Standards Institute 2008) demonstrated that *Fusarium volatile* had a low MIC of 1 µg/mL against amphotericin B, voriconazole (1 µg/mL), and posaconazole (0.5 µg/mL), whereas the fungus had high MICs for fluconazole (>64 µg/mL), itraconazole (>16 µg/mL), isavuconazole (4 µg/mL), anidulafungin (>8 µg/mL), and micafungin (>8 µg/mL) (Table 2).

Taxonomy

Fusarium volatile Al-Hatmi, Sand.-Den., S.A. Ahmed & de Hoog, ***sp. nov.*** MycoBank MB831243. Figs 3, 4.

Etymology: Named after its supposedly airborne entry in the human patient.

Typus: **French Guiana**, Cayenne, bronchoalveolar lavage (BAL) effusion of patient with lung infection, 2017, *M. Demar* (**holotype** CBS H-24004, culture ex-type CBS 143874).

Mycelium consisting of hyaline, smooth, branched, 1.5–5.5 µm diam hyphae. *Aerial conidiophores* erect, often reduced to conidiogenous cells, borne laterally on hyphae, less commonly irregularly or verticillately branched, up to 80 µm long, rarely proliferating, bearing terminal single mono- and polyphialides; *aerial phialides* subulate to subcylindrical, smooth- and thin-walled, (7–)11.5–21(–29) × 2–4.5 µm (av. 16.2 × 3.3 µm), commonly bearing a single conidiogenous locus, rarely polyphialidic, lacking noticeable periclinal thickening or collarettes; *aerial conidia* ellipsoid, allantoid, club-shaped to somewhat cylindrical, often with a flattened base, straight or gently curved, smooth- and thin-walled, 0–2(–3)-septate, (4.5–)5.5–19(–30) × (1.5–)2–4(–5.5) µm (av. 12.4 × 3.1 µm), grouped in moderately long, straight or flexuous chains, quickly collapsing to form discrete conidial heads; microcyclic conidiation present. *Sporodochia* produced infrequently in the aerial mycelium, rarely on the surface of carnation leaves, tan

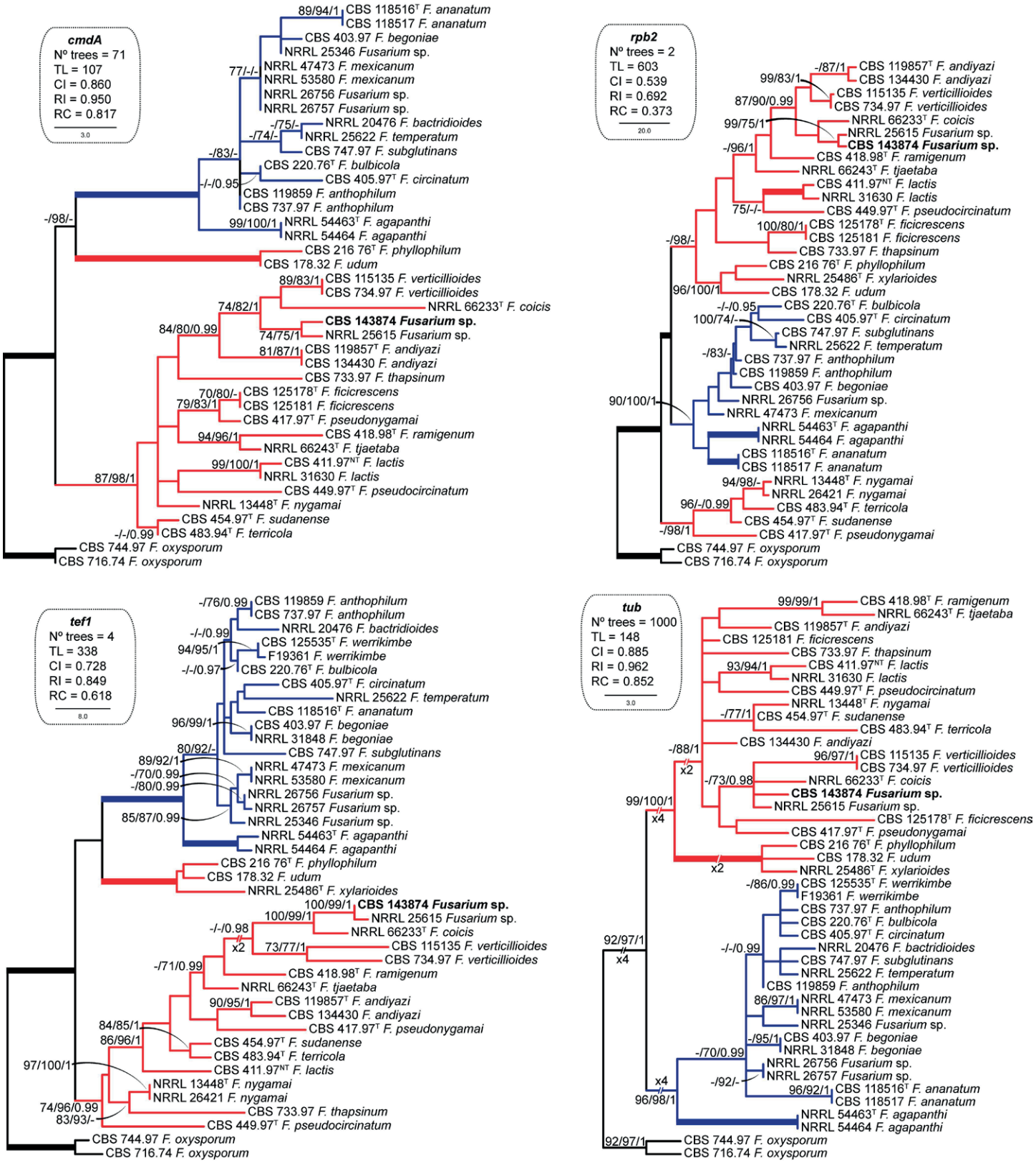

Fig. 1. Maximum Parsimony (MP) trees obtained from the individual phylogenetic analyses of the *cmdA*, *rpb2*, *tef1* and *tub* datasets of representative isolates of the *Fusarium fujikuroi* species complex. Numbers on the nodes are MP and Maximum-Likelihood (ML) bootstrap values (BS) above 70 % and Bayesian posterior probability values (PP) above 0.95. Thickened branches indicate full statistical support (MP-BS, ML-BS = 100 % and PP = 1). Coloured branches indicate the African (red) and American (blue) clades according to O'Donnell *et al*. (1998). The clinical isolate is highlighted in **bold**. Ex-type and ex-neotype strains are indicated with ^{T} and ^{NT}, respectively. The trees are rooted with *Fusarium oxysporum* CBS 744.97 and CBS 716.74. TL = tree length, CI = consistency index, RI = retention index, RC = rescaled consistency index.

to pale orange; *sporodochial conidiophores* simple or sparingly irregularly branched, 16–21(–22) × (3–)3.5–4.5 µm (av. 18.6 × 3.8 µm), bearing terminal and lateral single monophialides or terminal whorls of up to 4 monophialides; *sporodochial phialides* doliiform to subcylindrical, smooth- and thin-walled, (9.5–)11–15(–19) × (2.5–)3–4(–4.5) µm (av. 12.9 × 3.6 µm),

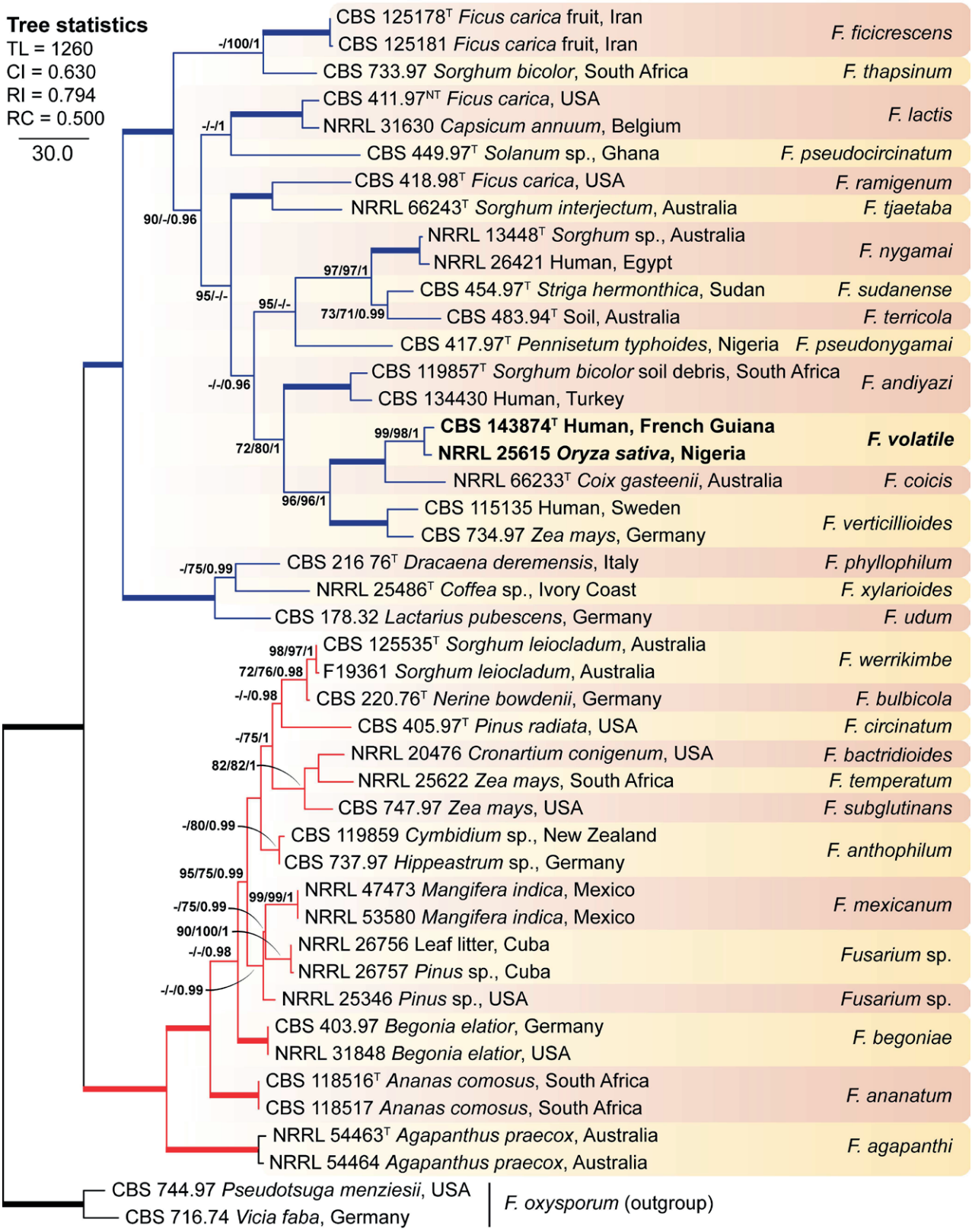

Fig. 2. The first of 16 most parsimonious trees obtained from the combined *cmdA*, *rpb2*, *tef1* and *tub* sequences of 43 strains belonging to the *Fusarium fujikuroi* species complex (FFSC). Numbers on the nodes are MP and Maximum-Likelihood (ML) bootstrap values (BS) above 70 % and Bayesian posterior probability values (PP) above 0.95. Thickened branches indicate full statistical support (MP-BS, ML-BS = 100 % and PP = 1). Coloured branches indicate the African (red) and American (blue) clades according to O'Donnell *et al.* (1998). Isolates and name of the new species are highlighted in **bold**. Ex-type and ex-neotype strains are indicated with ^{T} and ^{NT}, respectively. The tree is rooted with *Fusarium oxysporum* CBS 744.97 and CBS 716.74. TL = tree length, CI = consistency index, RI = retention index, RC = rescaled consistency index.

Fig. 3. *Fusarium volatile* (ex-type CBS 143874). **A–C.** Colonies (left obverse, right reverse) on MEA, PDA and OA, respectively, after 14 d at 24 °C. **D–H.** Aerial conidiophores and chains of conidia. **I–L.** Aerial phialides. **M.** Sporodochial phialides. **N.** Aerial conidia showing microcyclic conidiation. **O, P.** Aerial conidia. **Q.** Sporodochial conidia. Scale bars: **D–H** = 20 µm, **I–L** = 5 µm, all others = 10 µm.

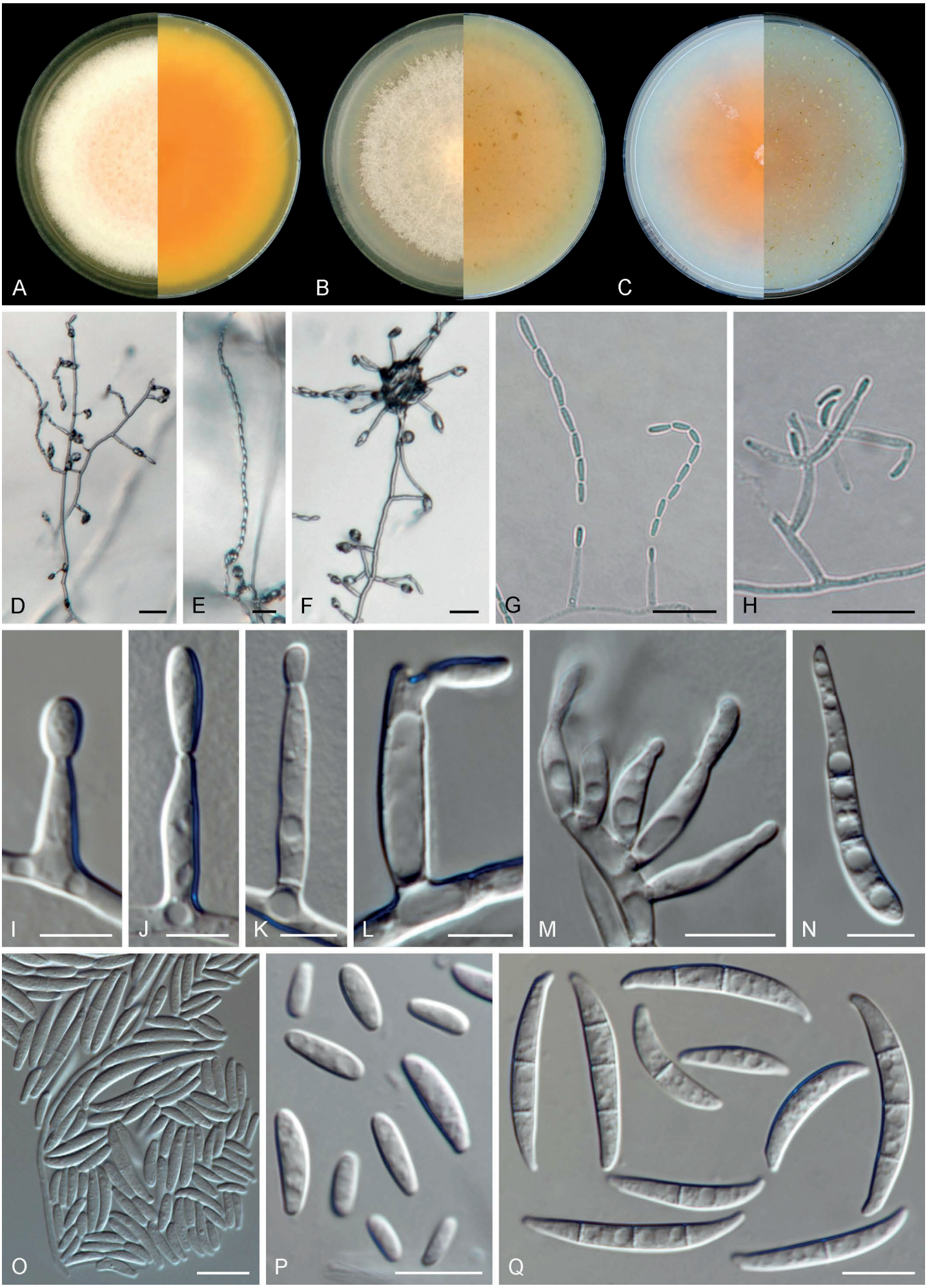

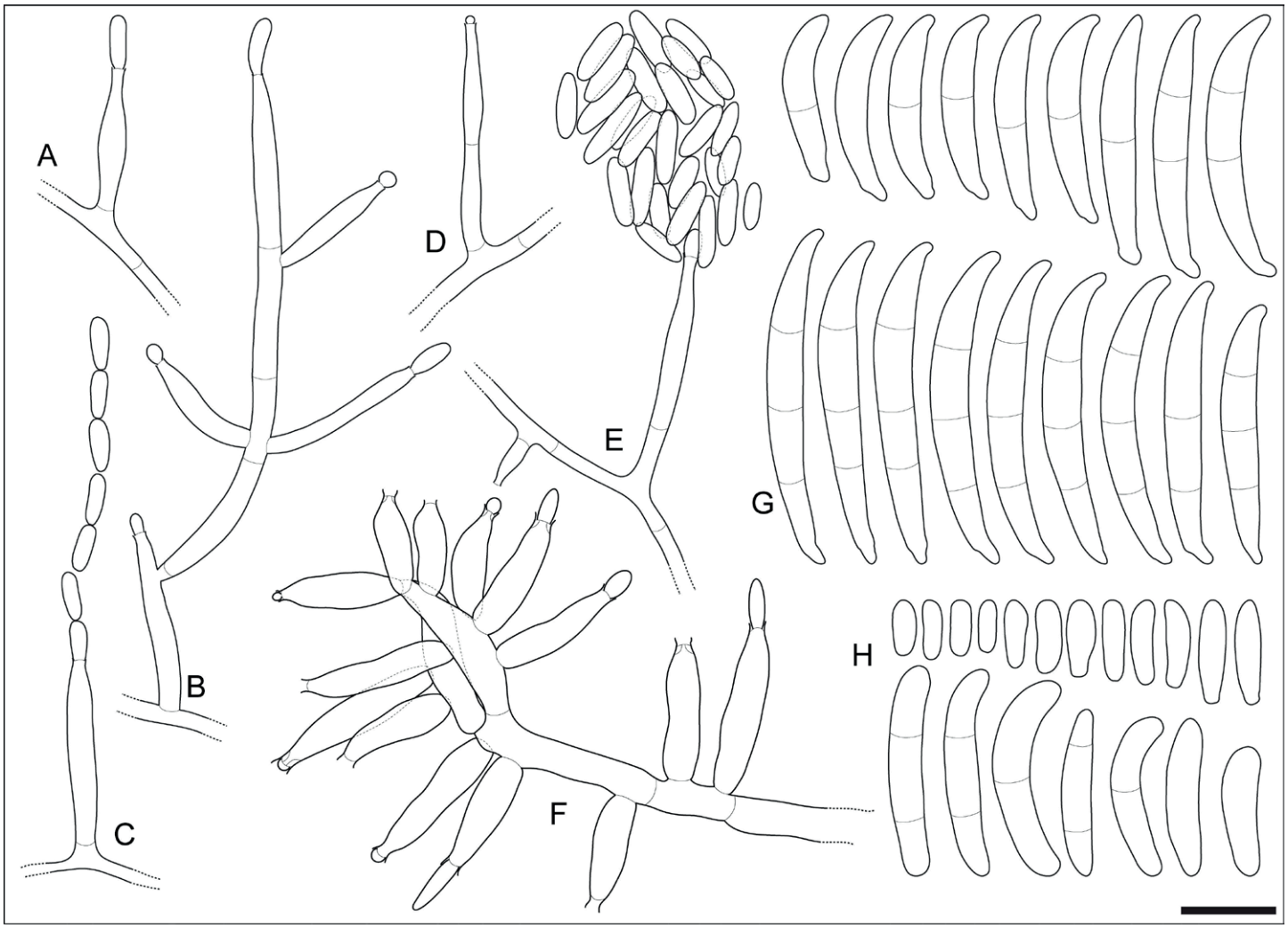

Fig. 4. *Fusarium volatile* (ex-type CBS 143874). **A–E.** Aerial conidiophores. **F.** Sporodochial conidiophore. **G.** Sporodochial conidia. **H.** Aerial conidia. Scale bar = 10 µm.

sporodochial conidia falcate, straight or dorsiventrally curved, curvature often more distinctly pronounced on the dorsal line, tapering toward the basal part; apical cell conical and slightly hooked; basal cell foot-shaped, (0–)1–3-septate, hyaline, thin- and smooth-walled. Aseptate conidia (14–)15–20.5 × 3–4 µm (av. 17.8 × 3.5 µm), 1-septate conidia (17–)19–24.5(–27) × (2–)3–4 µm (av. 21.7 × 3.5 µm), 2-septate conidia (26–)27–30(–31) × 3.5–4 µm (av. 28.4 × 3.9 µm), 3-septate conidia (27–)29–34.5(–36.5) × (3–)3.5–4(–4.5) µm (av. 31.7 × 4 µm); overall (14–)21–32.5(–36.5) × (2–)3–4.5 µm (av. 26.6 × 3.8 µm). *Chlamydospores* not observed.

Colonies growing in the dark after 7 d at 24 °C. On MEA reaching 50–68 mm diam, white, salmon to peach; colony surface raised to slightly umbonate, velvety felty; margin undulate to filiform; reverse orange to luteous with pale luteous periphery. On OA reaching 65–74 mm diam, saffron to rosy buff, turning pale vinaceous toward the periphery, membranous; margin entire with abundant submerged mycelium; reverse saffron to salmon, pale orange at the centre. On PDA with an average radial growth rate of 4.7–5.7 mm/d, reaching 60–80 mm diam, salmon, saffron to pale ochraceous with peach centre; flat with slightly raised centre, felty to cottony; margin irregular, undulate to lobate; reverse pale orange to ochraceous.

Cardinal growth temperatures: optimal development at 27–33 °C, minimum 18 °C, maximum 37 °C. The species was still able to grow at 37 °C, but not at 40 °C.

Notes: *Fusarium volatile* is phylogenetically closely related to *F. coicis* and *F. verticillioides*. The three mentioned species share the common morphological features attributed to the FFSC, such as the lack of chlamydospores, formation of oval to clavate microconidia and presence of monophialides, while sporodochia are not commonly produced. However, *F. coicis* and *F. volatile* differ significantly from *F. verticillioides* by having up to 3-septate microconidia (usually aseptate in *F. verticillioides*) and the additional presence, although rare, of polyphialides and microconidia formed on false heads and chains (strictly monophialidic, forming chains of conidia in *F. verticillioides*; Leslie & Summerell 2006). *Fusarium volatile* differs from *F. coicis* by its much shorter and less septate, curved macroconidia (up to 123 µm long, 4–10-septate and almost straight in *F. coicis*; Laurence *et al.* 2015).

Key to species of the *Fusarium fujikuroi* species complex known from human clinical specimens

1.	Polyphialides present	2
1	Polyphialides absent	6
2.	Microconidial chains present	3
2.	Microconidial chains absent	8
3.	Sporodochia orange	4
3.	Sporodochia tan to pale orange	10
4.	Chlamydospores present	*F. nygamai*
4.	Chlamydospores absent	5
5.	Pyriform conidia present	*F. fujikuroi*
5.	Pyriform conidia absent	*F. ramigenum*
6.	Napiform conidia present	7
6.	Napiform conidia absent	11
7.	Chlamydospores present	*F. napiforme*
7.	Chlamydospores absent	*F. thapsinum*
8.	Conidiophores mainly prostrate, rarely branched	9
8.	Conidiophores mainly erect, branched	13
9.	Chlamydospores present, polyphialides rare	*F. acutatum*
9.	Chlamydospores absent, polyphialides abundant and proliferating extensively	*F. sacchari*
10.	Microconidia 0-septate; macroconidia 3–5-septate, straight or almost so	*F. proliferatum*
10.	Microconidia 0–2(–3)-septate; macroconidia 0-3-septate, gently curved	*F. volatile*
11.	Microconidia in chains only	*F. verticillioides*
11.	Microconidia in head and chains	12
12.	Macroconidia present, 3–6-septate	*F. andiyazi*
12.	Macroconidia absent	*F. musae*
13.	Globose microconidia present	*F. anthophilum*
13.	Globose microconidia absent	14
14.	Colonies on PDA orange	15
14.	Colonies on PDA purple or violet	16
15.	Macroconidia formed only on aerial mycelium, sporodochia not produced	*F. ananatum*
15.	Macroconidia formed on sporodochia	*F. temperatum*
16.	Microconidia 0-septate, macroconidia rare or absent	*F. guttiforme*
16.	Microconidia 0–1-septate, macroconidia abundant	*F. subglutinans*

DISCUSSION

Fusariosis is usually acquired by inhalation of conidia or after trauma, skin burns, or sometimes through central venous access, or at lower incidence the gastrointestinal tract after consumption of contaminated food (Carneiro *et al*. 2011, Muhammed *et al*. 2011). *Fusarium* species can affect humans either by infection (Al-Hatmi *et al*. 2016b) or by mycotoxicosis (Marasas *et al*. 1984). Clinically, a disseminated fusariosis is characterised by persistent sepsis despite broad-spectrum antibiotic therapy. Although all organs may be concerned, cutaneous involvement is predominant, followed by pulmonary infection. Given that they are widespread in natural and human-made environments, *Fusarium* species may contaminate laboratory specimens and yield false-positive responses. The interpretation of *Fusarium* growth from clinical materials strongly depends on the clinical context (Nucci & Anaissie 2007). However, repeated isolation of the fungus and culture from sinus aspirate or deep respiratory secretions in severely immunocompromised hosts should always be considered as diagnostic of fusariosis (Nucci & Anaissie 2007).

In our study, we isolated a novel *Fusarium* species from broncho-alveolar lavage (BAL) aspirate. We cannot definitively differentiate between a fungal colonisation or an environmental contamination as the novel species was isolated in a single BAL sample and as the patient did not have any pulmonary clinical symptoms and evolved positively without antifungal treatment. Nevertheless, the chest radiography suggested the presence of an aspergilloma, given a suspicious image compatible with a Monod sign into the pulmonary cavern that could have been attributed to the presence of *Fusarium*, as deep infections by *Fusarium* and *Aspergillus* spp. may be confused. These opportunists present similar radiologic results, share comparable histologic appearances with hyaline, septate, branched hyphae and can cause similar clinical syndromes (Hayden *et al.* 2003). It is, therefore, important to make the correct diagnosis to optimise treatment and improve prognosis. Similarly, the correct species-level identification for *Fusarium* infections is crucial for a positive outcome since different infectious species may present marked differences in their antifungal susceptibility patterns, at least *in vitro* (Al-Hatmi *et al*. 2015).

Our phylogenetic analysis based on a four gene dataset (*cmdA*, *rpb2, tef* and *tub*) showed that *F. volatile* belongs to the FFSC, where it formed a genetically exclusive, strongly supported monophyletic clade, phylogenetically related to *F. coicis* and *F. verticillioides*. The phylogenetic clade representing *F. volatile* had already been recognised as a distinct species in FFSC, however, it was not formally described as such (O'Donnell *et al*. 2000). The FFSC is a species-rich group, currently comprising more than 50 taxa, including opportunists on humans, economically relevant plant pathogens, and mycotoxin producers. Most of these species have been recognised based on phylogenetic analyses (Kvas *et al*. 2009). A large number of cryptic, unnamed

phylogenetic species remain to be formally described. Based on phylogenetic relationships, O'Donnell *et al*. (1998) organised the FFSC into three main clades (African, American and Asian clades), each encompassing numerous species with similar biogeographic patterns. Our results showed that, despite being isolated in South America, *F. volatile* clusters in the African clade, which matches with the African origin of a genetically identical strain (NRRL 25615) from Nigeria. Interestingly, our individual phylogenies do not support the current delimitation of the African clade of FFSC, which was found to be polyphyletic using *cmdA*, *rpb2* and *tef1* markers. The phylogenies support the results previously reported by other authors using the same and additional phylogenetic markers (Kvas *et al*. 2009, Walsh *et al*. 2010, O'Donnell *et al*. 2013, Laurence *et al*. 2015, Sandoval-Denis *et al*. 2018), which shows that the biogeographic clade distribution of the FFSC needs further re-valuation.

The voucher strain CBS 143874 of *F. volatile* clusters as a sister clade to *F. coicis* and *F. verticillioides,* the latter species being known to be capable of causing human infection (Al-Hatmi *et al.* 2016b). *Fusarium verticillioides* is an important producer of mycotoxins, including fumonisins (Leslie & Summerell 2006, Rosa Junior *et al.* 2019); these toxins are highly detrimental to animals and are suspected to be responsible for acute and chronic human diseases (Leslie & Summerell 2006). In contrast, *F. coicis* is known only from *Coix gasteenii* (*Poaceae*), a rare Australian grass species, while no human infection or toxin production has been reported. These clinical data suggest that the new species *F. volatile* is unlikely a primary human pathogen but rather an opportunist that takes advantage of the host's compromised immune response. Production of mycotoxins, however, was not tested in *F. volatile* and remains to be studied.

Among the FFSC species known to occur on humans (de Hoog *et al.* 2019), *F. volatile* is morphologically similar to *F. fujikuroi*, *F. nygamai*, *F. proliferatum* and *F. ramigenum*. All the latter species are characterised by obovoid to clavate microconidia formed in false heads and chains from mono- and polyphialides, and by, except *F. nygamai*, absence of chlamydospores. *Fusarium volatile* can be recognised by its ellipsoid to cylindrical microconidia (*vs*. the pyriform microconidia of *F. fujikuroi* and *F. proliferatum*, and the obovoid microconidia of *F. ramigenum*), its less-septate macroconidia (up to 3-septate *vs*. up to 5-septate in all the species listed above), and its tan to pale orange sporodochia (orange in *F. fujikuroi* and *F. nygamai*) (Leslie & Summerell 2006). Two additional opportunistic species on humans, *F. acutatum* and *F. sacchari*, produce microconidia only on false heads, but might also be confused with *F. volatile* because of their similar morphology and septation of macroconidia. *Fusarium volatile* differs from *F. acutatum* by its 0–3-septate microconidia (0-septate in the latter species) and its less curved macroconidia. It can be separated from *F. sacchari* by the microconidial shape (oval in *F. sacchari*), while polyphialides are rarely seen in *F. volatile* (common in *F. sacchari*).

Antifungal susceptibility testing demonstrated that *F. volatile* had reduced MICs for posaconazole (0.5 µg/mL), followed by amphotericin B and voriconazole (1 µg/mL), whereas MIC values for fluconazole, isavuconazole, itraconazole and the echinocandins were elevated (Table 2). In the present case, no antifungal therapy was given. In general, *Fusarium* spp. show a remarkably high degree of intrinsic resistance to a wide spectrum of clinically available antifungal drugs. Prior to the voriconazole era, the initial approach of treating invasive fusariosis consisted on the administration of high-dose (>5 mg/kg/d) liposomal amphotericin B (Al-Hatmi *et al*. 2017). After FDA approval in 2002, voriconazole has become the first-line treatment because of its lower toxicity and higher clinical efficacy against fusariosis (Walsh *et al*. 1998, Stempel *et al*. 2015). The European Fungal Infection Study Group and the European Confederation of Medical Mycology recommended a lipid formulation of amphotericin B or voriconazole for treating invasive fusariosis (Tortorano *et al.* 2014).

In conclusion, we described the new species *F. volatile*, belonging to the FFSC. This new taxon was found in a BAL sample from a patient with non-haematological predisposing conditions. Further studies are required to determine natural ecology, transmission routes and the potential pathogenic role of this new species.

REFERENCES

Al-Hatmi AM, Bonifaz A, Ranque R, *et al*. (2017). Current antifungal treatment of fusariosis. *International Journal of Antimicrobial* **51**: 326–332.

Al-Hatmi AM, van Diepeningen AD, Curfs-Breuker I, *et al.* (2015). Specific antifungal susceptibility profiles of opportunists in the *Fusarium fujikuroi* complex. *Journal of Antimicrobial Chemotherapy* **70**: 1068–1071.

Al-Hatmi AMS, Hagen F, Menken SBJ, *et al*. (2016a). Global molecular epidemiology and genetic diversity of *Fusarium*, a significant emerging human opportunist from 1958-2015. *Emerging Microbes and Infections* **5**: e124.

Al-Hatmi AMS, Meis JF, de Hoog GS (2016b). *Fusarium*: molecular diversity and intrinsic drug resistance. *PLoS Pathogens* **12**: e1005464.

Aoki T, Smith JA, Mount LL, *et al*. (2013). *Fusarium torreyae sp. nov.*, a pathogen causing canker disease of Florida torreya (*Torreya taxifolia*), a critically endangered conifer restricted to northern Florida and southwestern Georgia. *Mycologia* **105**: 312–319.

Carneiro HA, Coleman JJ, Restrepo A, *et al*. (2011). *Fusarium* infection in lung transplant patients: Report of 6 cases and review of the literature. *Medicine* **90**: 69–80.

Chilaka CA, De Boevre M, Atanda OO, *et al*. (2017). The status of *Fusarium* mycotoxins in sub-Saharan Africa: A review of emerging trends and post-harvest mitigation strategies towards food control. *Toxins* **9**: 19.

De Hoog GS, Guarro J, Gené J, *et al*. (2019). Atlas of Clinical Fungi, 4th ed. Westerdijk Institute / Universitat Rovira i Virgili, Utrecht / Reus.

Edwards J, Auer D, de Alwis SK, *et al*. (2016). *Fusarium agapanthi sp. nov.*, a novel bikaverin and fusarubin-producing leaf and stem spot pathogen of *Agapanthus praecox* (African lily) from Australia and Italy. *Mycologia* **108**: 981–992.

Fisher NL, Burguess LW, Toussoun TA, *et al*. (1982). Carnation leaves as a substrate and for preserving cultures of *Fusarium* species. *Phytopathology* **72**: 151–153.

Geiser DM, Jiménez-Gasco M, Kang S (2004). FUSARIUM-ID v. 1.0: a DNA sequence database for identifying *Fusarium*. *European Journal of Plant Pathology* **110**: 473–479.

Glass NL, Donaldson GC (1995). Development of primer sets designed for use with the PCR to amplify conserved genes from filamentous ascomycetes. *Applied and Environmental Microbiology* **61**: 1323–1330.

Guarro J (2013). Fusariosis, a complex infection caused by a high diversity of fungal species refractory to treatment. *European Journal of Clinical Microbiology & Infectious Diseases* **32**: 1491–1500.

Hayden RT, Isotalo PA, Parrett T, *et al*. (2003). In situ hybridization for the differentiation of *Aspergillus*, *Fusarium,* and *Pseudallescheria* species in tissue section. *Diagnostic Molecular Pathology* **12**: 21–26.

Kvas M, Marasas WFO, Wingfield BD, *et al*. (2009). Diversity and evolution of *Fusarium* species in the *Gibberella fujikuroi* complex. *Fungal Diversity* **34**: 1–21.

Laurence MH, Walsh JL, Shuttleworth LA, *et al*. (2015). Six novel species of *Fusarium* from natural ecosystems in Australia. *Fungal Diversity* **77**: 349–366.

Leslie JF, Summerell BA (2006). The *Fusarium* laboratory manual. Blackwell Publishing, Ames.

Liu YJ, Whelen S, Hall BD (1999). Phylogenetic relationships among ascomycetes: evidence from an RNA polymerse II subunit. *Molecular Biology and Evolution* **16**: 1799–1808.

Marasas WFO, Nelson PE, Toussoun TA (1984). Toxigenic *Fusarium* species. Identity and mycotoxicology. The Pennsylvania State University Press, USA.

Miller MA, Pfeiffer W, Schwartz T (2012). The CIPRES science gateway: enabling high-impact science for phylogenetics researchers with limited resources. In: Proceedings of the 1st Conference of the Extreme Science and Engineering Discovery Environment: Bridging from the extreme to the campus and beyond: 1–8. Association for Computing Machinery, USA.

Muhammed M, Coleman JJ, Carneiro HA, *et al*. (2011). The challenge of managing fusariosis. *Virulence* **2**: 91–96.

Nirenberg HI (1976). Untersuchungen über die morphologische und biologische Differenzierung in der *Fusarium*-Sektion Liseola. *Mitteilungen der Biologischen Bundesanstalt für Land- und Forstwirtschaft Berlin-Dahlem* **169**: 1–117.

Nirenberg HI, O'Donnell K (1998). New *Fusarium* species and combinations within the *Gibberella fujikuroi* species complex. *Mycologia* **90**: 434–458.

Nucci M, Anaissie E (2007). *Fusarium* infections in immunocompromised patients. *Clinical Microbiology Reviews* **20**: 695–704.

Nylander JAA (2004). *MrModeltest v2*. Program distributed by the author.

O'Donnell K, Cigelnik E, Nirenberg HI (1998). Molecular systematics and phylogeography of the *Gibberella fujikuroi* species complex. *Mycologia* **90**: 465–493.

O'Donnell K, Nirenberg HI, Aoki T, *et al*. (2000). A multigene phylogeny of the *Gibberella fujikuroi* species complex: detection of additional phylogenetically distinct species. *Mycoscience* **41**: 61–78.

O'Donnell K, Rooney AP, Proctor RH, *et al*. (2013). Phylogenetic analyses of RPB1 and RPB2 support a middle Cretaceous origin for a clade comprising all agriculturally and medically important fusaria. *Fungal Genetics and Biology* **52**: 20–31.

O'Donnell K, Ward TJ, Robert VARG, *et al*. (2015). DNA sequence-based identification of *Fusarium*: Current status and future directions. *Phytoparasitica* **43**: 583–595.

O'Donnell K, Sutton DA, Rinaldi MG, *et al*. (2009b). Novel multilocus sequence typing scheme reveals high genetic diversity of human pathogenic members of the *Fusarium incarnatum* - *F. equiseti* and *F. chlamydosporum* species complexes within the United States. *Journal of Clinical Microbiology* **47**: 3851–3861.

Rayner RW (1970). A mycological colour chart. CMI and British Mycological Society, Kew, Surrey.

Ronquist F, Huelsenbeck JP (2003). MrBayes 3: Bayesian phylogenetic inference under mixed models. *Bioinformatics* **19**: 1572–1574.

Rosa Junior OF, Dalcin MS, Nascimento VL, *et al*. (2019). Fumonisin production by *Fusarium verticillioides* in maize genotypes cultivated in different environments. *Toxins* **11**: 215.

Sandoval-Denis M, Guarnaccia V, Polizzi G, *et al*. (2018). Symptomatic Citrus trees reveal a new pathogenic lineage in *Fusarium* and two new *Neocosmospora* species. *Persoonia* **40**: 1–25.

Sandoval-Denis M, Swart WJ, Crous PW (2018). New *Fusarium* species from the Kruger National Park, South Africa. *MycoKeys* **34**: 63–92.

Stamatakis A (2014). RAxML version 8: a tool for phylogenetic analysis and post-analysis of large phylogenies. *Bioinformatics* **30**: 1312–1313.

Stempel JM, Hammond SP, Sutton DA, *et al* (2015). Invasive fusariosis in the voriconazole era: Single-center 13-year experience. *Open Forum Infectious Diseases* **2**: ofv099.

Sung GH, Sung JM, Hywel-Jones NL, *et al*. (2007). A multi-gene phylogeny of *Clavicipitaceae* (Ascomycota, Fungi): Identification of localized incongruence using a combinational bootstrap approach. *Molecular Phylogenetics and Evolution* **44**: 1204–1223.

Swofford DL (2003). PAUP*. Phylogenetic Analysis Using Parsimony (*and other methods). Version 4. Sinauer Associates, Sunderland, Massachusetts, USA.

Tortorano AM, Richardson M, Roilides E, *et al*. (2014). ESCMID and ECMM joint guidelines on diagnosis and management of hyalohyphomycosis: *Fusarium* spp., *Scedosporium* spp. and others. *Clinical Microbiology and Infection* **3**: 27–46.

Walsh J, Laurence M, Liew E, *et al*. (2010). *Fusarium*: two endophytic novel species from tropical grasses of northern Australia. *Fungal Diversity* **44**: 149–159.

Walsh TJ, Hiemenz JW, Seibel NL, *et al*. (1998). Amphotericin B lipid complex for invasive fungal infections: analysis of safety and efficacy in 556 cases. *Clinical Infectious Diseases* **26**: 1383–1396.

Wingfield, MJ, de Beer ZW, Slippers B, *et al*. (2012). One fungus, one name promotes progressive plant pathology. *Molecular Plant Pathology* **13**: 604–613.